



Gas loss and isotopic fractionation induced by pumping during ice core gas extractions

Qiuyu Li¹, Huanting Hu^{1, *}, Guitao Shi², Danhe Wang^{2,3}, Zhe Li², Shugui Hou¹

¹Key Laboratory of Polar Ecosystem and Climate Change, Ministry of Education, School of Oceanography, Shanghai Jiao Tong University, 1954 Huashan Road, Shanghai 200030, China

²Key Laboratory of Geographic Information Science (Ministry of Education), School of Geographic Sciences and State Key Laboratory of Estuarine and Coastal Research, East China Normal University, Shanghai, 200241, China

³Key Laboratory of Polar Science, Ministry of Natural Resources, Polar Research Institute of China, Shanghai 200136, China

Correspondence to: Huanting Hu (huanting.hu@sjtu.edu.cn)

10 **Abstract.** Ice core trapped gases are crucial paleoclimate archives, yet various gas loss processes introduce fractionation that obscures climatic signals. Among these, fractionation induced by pumping during sample evacuation has remained poorly constrained. Here we quantify pump-induced fractionation through controlled pumping experiments on a horizontal ice core from coastal East Antarctica. We investigated the responses of gas ratios and isotopic compositions ($\delta^{18}\text{O}_{\text{atm}}$, $\delta\text{O}_2/\text{N}_2$ and $\delta\text{Ar}/\text{N}_2$) to varied rotary or turbo pumping durations (0.5 – 90 min). We found that the extent of gas loss is pump-dependent (turbo > rotary) but independent of pumping duration. The $\delta\text{Ar}/\text{N}_2 - \delta\text{O}_2/\text{N}_2$ fractionation slope from pair differences between samples subjected to different pumping durations was 0.86, significantly higher than the ≤ 0.5 slopes typical of bubble close-off and post-coring gas loss, and approaching the slope of ~ 1 characteristic of size-dependent gas diffusion in ice lattice. Isotopic enrichment in $\delta^{18}\text{O}_{\text{atm}}$ correlated strongly with gas loss magnitude, yielding fractionation slopes of $-0.0132\text{‰}\cdot\text{‰}^{-1}$ against $\delta\text{O}_2/\text{N}_2$ and $-0.0124\text{‰}\cdot\text{‰}^{-1}$ against $\delta\text{Ar}/\text{N}_2$, substantially steeper than those associated with natural gas loss processes. These observations imply that pumping preferentially evacuates gases from ice cracks, which are mainly influenced by mass-dependent fractionation, leaving bubble-resident gases fractionated by lattice diffusion. The coupled loss of O_2 and Ar insights corrections for $\delta^{18}\text{O}_{\text{atm}}$ and $\delta\text{O}_2/\text{N}_2$ based on the covariations among $\delta^{18}\text{O}_{\text{atm}}$, $\delta\text{O}_2/\text{N}_2$ and $\delta\text{Ar}/\text{N}_2$. Application to the Dome Fuji ice core demonstrates that scatter in $\delta\text{O}_2/\text{N}_2$ records from the bubble-clathrate transition zone can be effectively reduced by correcting for gas losses using $\delta\text{Ar}/\text{N}_2$ as a proxy. Our findings provide the first quantitative constraints on pump-induced fractionation and offer a feasible correction method for reducing data uncertainties, thereby enhancing the fidelity of ice core paleoclimate reconstructions.

1 Introduction

Trapped gases in ice cores are primary archives for reconstructing paleoclimate and past atmospheric composition over the past million years (Severinghaus et al., 1998; Petit et al., 1999; Bender, 2002; Jouzel et al., 2007; Severinghaus et al., 2009; Yan et al., 2019; Shackleton et al., 2025). Among these, the O_2/N_2 ratios and the $^{18}\text{O}/^{16}\text{O}$ isotopic compositions of



trapped air are of particular interest: they correlate with summer insolation and are widely used for dating continuous ice cores (Landais et al., 2012; Extier et al., 2018). More recently, high-precision O_2/N_2 measurements from various ice cores have been employed to reconstruct the atmospheric oxygen concentrations (pO_2) over the Pleistocene (Stolper et al. 2016; Yan et al., 2021). However, trapped gases are subject to fractionation through several gas-loss processes, occurring during
35 bubble close-off, ice core drilling, storage, and laboratory trapped gas extraction (Sowers et al., 1989; Bender et al., 1995; Kawamura et al., 2007). For instance, using O_2/N_2 to reconstruct paleo- pO_2 requires rigorous correction for such fractionations to resolve the subtle ($\sim 0.7 \text{ ‰}$) decline in pO_2 over the past 800,000 years (Stolper et al., 2016). In old blue ice samples, which often have large age uncertainties, pO_2 is reconstructed from the deviations in intercepts of the $O_2/N_2 - Ar/N_2$ relationships. This method demands a strong linear correlation between O_2/N_2 and Ar/N_2 (Yan et al., 2021). Thus,
40 high-precision analysis of gas ratios and isotopic compositions of ice core trapped gases are fundamental to ice core dating, pO_2 reconstruction, and robust paleoclimate interpretation. Critically, gas loss compromises the integrity of ice core trapped gas records, increasing data scatter and introducing uncertainty into orbital tuning and paleoclimate reconstructions (Suwa and Bender, 2008; Landais et al., 2012). Despite the known impacts of natural gas loss, fractionation induced by pumping during trapped gas extraction has rarely been quantified. Addressing this gap is essential for improving the accuracy and
45 reliability of ice core gas proxies.

Gas loss processes alter the composition of trapped gases through two primary mechanisms: size-dependent and mass-dependent fractionation (Bender et al., 1995; Severinghaus and Battle, 2006). When O_2 and Ar escape from gas bubbles and diffuse through the ice lattice (Fig. 1), the fractionation is predominantly size-dependent and nearly mass-independent (Huber et al., 2006). This occurs because the molecular diameters of O_2 (3.467 Å) and Ar (3.542 Å) are smaller than the
50 critical size of ~ 3.6 Å for lattice diffusion. Meanwhile, larger molecules like N_2 (3.798 Å) remain largely unaffected (Reid et al., 1959; Huber et al., 2006). The apparent effect of size-dependent fractionation is depletion of O_2 and Ar in the trapped gas relative to air (Severinghaus and Battle, 2006; Kawamura et al., 2007). In comparison, mass-dependent fractionation dominates when gases diffuse through ice microcracks via Knudsen or molecular diffusion (Bender et al., 1995; Kobashi et al., 2008; Fig. 1). Lighter isotopes escape preferentially, enriching heavier isotopes (e.g., ^{18}O) in the remaining trapped gases
55 (Craig et al., 1988). Both size-dependent and mass-dependent fractionations are commonly observed in bubble close-off gas loss (BCGL) and post-coring gas loss (PCGL) (Bender et al., 1995; Severinghaus et al., 2009; Oyabu et al., 2021).

The characteristics of gas loss fractionation can be evaluated from the relationships between O_2/N_2 and Ar/N_2 gas ratios and the isotopic composition of trapped O_2 . In relevant studies, these parameters are expressed in δ notation, defined as:

$$\delta = \left(\frac{R_{\text{sample}}}{R_{\text{standard}}} - 1 \right) \times 1000 \quad (1)$$

60 where δ can represent $\delta^{15}N$, $\delta^{18}O$, $\delta O_2/N_2$ or $\delta Ar/N_2$. R_{sample} is the ratio of different isotopes or elements in a given sample (e.g., $^{18}R = ^{18}O/^{16}O$, or R_{O_2/N_2} is the gas ratio of O_2/N_2), and R_{standard} is the equivalent ratio of modern air.

Size-dependent and mass-dependent fractionations produce distinct slopes in the relationships between $\delta Ar/N_2$ and $\delta O_2/N_2$ (Severinghaus et al., 2009; Oyabu et al., 2021). As O_2 and Ar have similar molecular diameters, size-dependent gas



loss yields a $\delta\text{Ar}/\text{N}_2 - \delta\text{O}_2/\text{N}_2$ slope of ~ 1 for the residual gas (Fig. 1), without significant isotopic fractionation (Ikeda-
 65 Fukazawa et al., 2005; Severinghaus and Battle, 2006; Oyabu et al., 2021). In contrast, mass-dependent gas diffusion along
 ice cracks to the exterior scales with the mass or pressure difference of gas molecules, resulting in a $\delta\text{Ar}/\text{N}_2 - \delta\text{O}_2/\text{N}_2$ slope of
 ~ 3 (Severinghaus and Battle, 2006; Severinghaus et al., 2009). For BCGL, the combined effect of these fractionations
 results in an apparent $\delta\text{Ar}/\text{N}_2 - \delta\text{O}_2/\text{N}_2$ slope of ~ 0.5 (Craig et al., 1988; Sowers et al., 1989; Kobashi et al., 2008;
 Severinghaus et al., 2009; Oyabu et al., 2021). For PCGL, available data suggest that $\delta\text{Ar}/\text{N}_2 - \delta\text{O}_2/\text{N}_2$ slopes range from 0.22
 70 to 0.54 (Oyabu et al., 2021). For ice cores stored at higher temperatures ($> -50^\circ\text{C}$) or for long storage time, the
 $\delta\text{Ar}/\text{N}_2 - \delta\text{O}_2/\text{N}_2$ slope may fall below 0.5, as observed in the Dome C, Byrd and outer ice of the Dome Fuji ice cores (Bender
 et al., 1995; Oyabu et al., 2021). The Tibetan Chongce ice core also exhibits a low $\delta\text{Ar}/\text{N}_2 - \delta\text{O}_2/\text{N}_2$ slope of 0.29, attributed
 to additional O_2 consumption by respiration alongside gas losses (Hu et al., 2022). In the bubble-clathrate transition zone
 (BCTZ), however, gas diffusion from bubbles to clathrates reveals a $\delta\text{Ar}/\text{N}_2 - \delta\text{O}_2/\text{N}_2$ slope close to 1 (Seltzer et al., 2017;
 75 Severinghaus, 2019; Oyabu et al., 2021), indicating the dominance of size-dependent lattice diffusion. Overall, for bubbly
 ice, BCGL and PCGL typically produce $\delta\text{Ar}/\text{N}_2 - \delta\text{O}_2/\text{N}_2$ slopes close to or below 0.5.

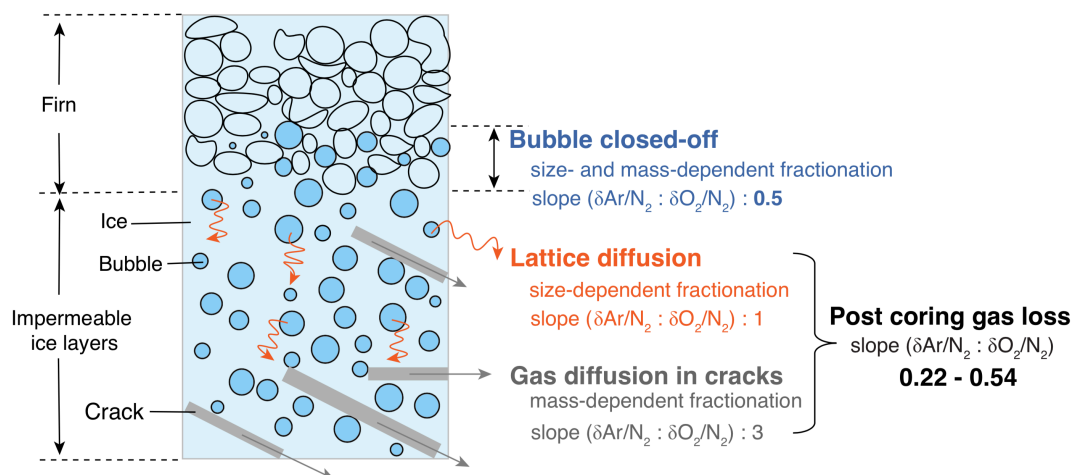


Figure 1: Schematic diagram of natural gas loss processes and their associated gas ratio slopes. Slopes for BCGL and PCGL are compiled from Oyabu et al. (2021)

80

Apart from BCGL and PCGL, mechanical disturbances induced by pumping on ice samples prior to gas extraction can also cause trapped gas losses (Kobashi et al., 2008). However, the fractionation associated with this pumping step remains poorly constrained. Ice core trapped gases are typically extracted using melt-equilibrium wet extraction (Sowers et al., 1997), ice crushing dry extraction (Andree et al., 1986; Wilson and Long, 1997), or sublimation extraction (Wilson and Donahue,
 85 1989). In the widely used wet extraction method for N_2 , O_2 , and noble gases, ice samples are first evacuated using rotary and turbo pumps to remove ambient air from the sample flask. The required evacuation time varies across laboratories and is often determined empirically. For example, Sowers et al. (1989) and Severinghaus et al. (2009) pumped ice samples for 1 h



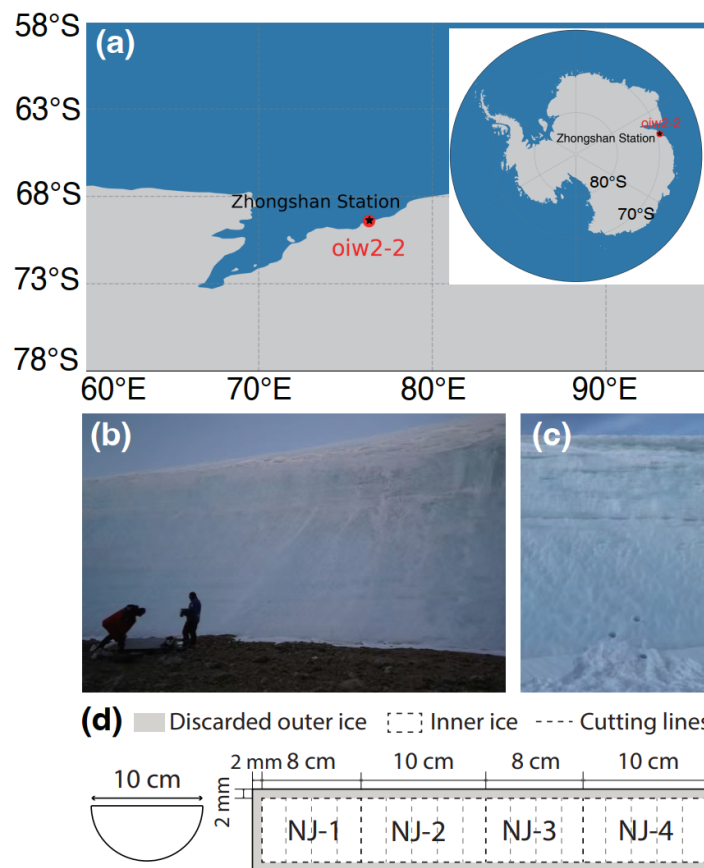
to reach pressures below 10^{-3} mbar. Higgins et al. (2015) and Severinghaus et al. (2003) pumped blue ice samples for 40 min to reach 10^{-3} mbar for Ar isotope and Kr/Xe analysis. More recently, Yan et al. (2019) shortened the evacuation time to 15
90 min to reduce potential gas loss. In our laboratory, the standard protocol involves evacuation for 0.5 min with a rotary pump until the pressure falls below 1 mbar, followed by switching to a turbo pump for 10 min to reach a final pressure of $\sim 10^{-5}$ mbar. Insufficient pumping may contaminate trapped gases with modern air, whereas excessive pumping may exacerbate gas loss from the ice. Fractured ice cores, such as the Siple Dome and the lower sections of the Allan Hills S27 ice core, has been shown to yield reduced data reproducibility, underscoring the need for optimized protocols (Severinghaus et al., 2009;
95 Yan et al., 2021). Yet, the specific fractionation patterns induced by pumping and their quantitative impact on trapped gas composition remain largely unconstrained, as pump effects are difficult to disentangle from PCGL.

To evaluate pump-induced gas loss fractionation, we conducted pumping experiments using a horizontal ice core drilled from coastal East Antarctica. We systematically varied pumping duration under rotary and turbo pumps and measured the resulting changes in trapped gas oxygen isotopic and gas ratio compositions ($\delta^{18}\text{O}_{\text{atm}}$, $\delta\text{O}_2/\text{N}_2$, $\delta\text{Ar}/\text{N}_2$). By examining the
100 slopes among these parameters, we characterize the fractionation signature unique to pump-induced gas loss. Finally, as a demonstration of paleoclimate relevance, we applied a $\delta\text{Ar}/\text{N}_2$ -based gas loss corrections to $\delta\text{O}_2/\text{N}_2$ data from the BCTZ of the Dome Fuji ice core. This approach offers a promising pathway to correct for gas loss artifacts in scattered datasets, thereby improving the precision of orbital dating and enhancing the fidelity of ice core paleoclimate records.

2 Materials and methods

105 2.1 Sampling information

In February 2020, a horizontal ice core (oiw2-2) was recovered from an ice stream on the Ingrid Christensen Coast, East Antarctica ($69^\circ 24' 29''$ S, $76^\circ 20' 46''$ E; 151 m a.s.l.; Fig. 2), using a hand auger. The length of the ice core was 100 cm, with a diameter of 10 cm (Fig. 2). After drilling, the ice core was stored in clean polyethylene bags with insulated cabinets and transported under freezing conditions (-20°C). The ice core was subsequently stored in a -50°C cold room at the East
110 China Normal University Environmental Stable Isotope Laboratory (ECNU-ESIL). In a -20°C walk-in cold room, the ice core was bisected with a bandsaw. One half (~ 50 cm long) was transported to Shanghai Jiao Tong University for trapped gas isotopic measurements and divided into four sections for pumping experiments, as shown in Fig. 2d.



115 **Figure 2:** Sampling Information. (a) Maps of the drilling site. (b) Diagram of the ice stream. (c) The borehole on the ice stream. (d) Ice core cutting plan for pumping experiments.

2.2 Trapped gas extraction and isotope measurements

Trapped gas extraction and isotope measurements were performed at the Shanghai Jiao Tong University Gas Stable Isotope Lab. For each analysis, ~10 g of ice was cut with a clean bandsaw in a -20 °C walk-in cold room. The outer 2 mm of each ice sample was trimmed off to eliminate potential modern air contamination.

120 Trapped gases were extracted and analyzed using a melt-equilibrium method following Emerson et al. (1995). Ice samples were placed in a sample flask connected to a vacuum line (Fig. 3). The flask bottom was immersed in an ethanol bath at -30 to -40 °C to prevent ice melting during pumping. The flask was first evacuated by a rotary pump (Pfeiffer Vacuum Duo 3) and then switched to a turbo pump (Pfeiffer Vacuum HiPace 80) after the pressure reached ≤ 1 mbar. The standard evacuation durations for preparing an ice sample were 0.5 and 10 min for the rotary and turbo pumps, respectively.

125 The sample flask would reach a final pressure of $\sim 10^{-5}$ to 10^{-6} mbar before sealing. The ice sample was then melted in a warm water bath, releasing the trapped gases into the headspace. These headspace gases were purified on the vacuum line



through two liquid nitrogen traps (-196°C) to remove water vapor and CO_2 . The purified mixture of N_2 , O_2 , and Ar was collected in a sample finger filled with silica gel (Sigma Aldrich, 45–60 mesh) at liquid nitrogen temperature. Finally, the sample gases were introduced into a dual-inlet Thermo Fisher Delta V Plus mass spectrometer for simultaneous analysis of isotopic compositions and gas ratios ($\delta^{15}\text{N}$, $\delta^{18}\text{O}$, $\delta\text{O}_2/\text{N}_2$ and $\delta\text{Ar}/\text{N}_2$). Long-term external precisions (1σ), established from 26 modern air samples collected outside the laboratory between August and December 2021, were $\pm 0.025\%$, $\pm 0.052\%$, $\pm 0.5\%$, and $\pm 0.5\%$ for $\delta^{15}\text{N}$, $\delta^{18}\text{O}$, $\delta\text{O}_2/\text{N}_2$, and $\delta\text{Ar}/\text{N}_2$, respectively.

The total air content (TAC) of this ice core was determined and calibrated from the gas pressure measured on the sample bellow of the mass spectrometer dual inlet system. The mean TAC was $0.06 \pm 0.01 \text{ scc}\cdot\text{g}^{-1}$ (standard cubic centimeters per gram, “standard” refers to 273 K and 101.325 kPa). Although this core was retrieved from an ice stream, the presence of visible gas bubbles and the relative high TAC values indicate that the ice underwent normal firn densification and bubble closure processes. This suggests that, despite its origin, the core retains physical characteristics comparable to those of deep ice cores and can serve as a suitable analogue for investigating gas-trapping processes and pump-induced artifacts in paleoclimate studies.

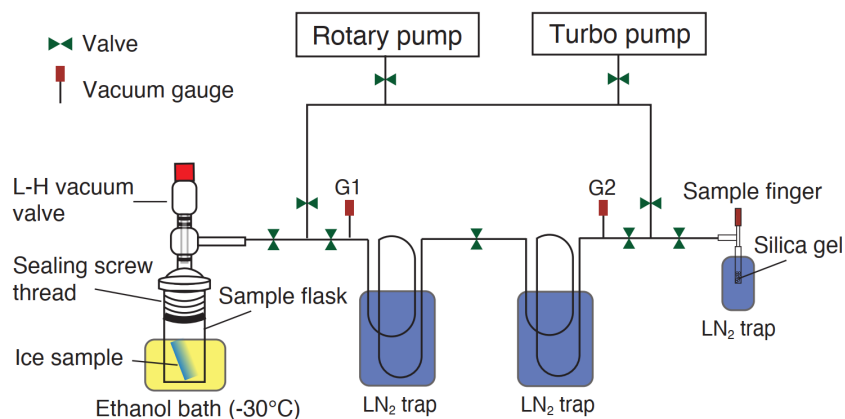


Figure 3: Schematic diagram of the vacuum line for ice core trapped gas extraction and purification. G1 and G2 are pressure gauges; LN_2 traps are cold traps at liquid nitrogen temperature (-196°C).

2.3 Pumping experiments

The pumping experiments were conducted by varying the evacuation duration for ice core samples under rotary or turbo pumps to evaluate pump-induced gas loss fractionation. The standard protocol (0.5 min rotary and 10 min turbo) was defined as the “initial sample” for each pumping experiment. We then increased the pumping duration for one pump type while holding the other as the same as the “initial sample”. The oiw2-2 ice core was divided into four sections for these experiments (Fig. 2d): NJ-1 and NJ-3 were used for rotary pumping experiments; NJ-2 and NJ-4 were used for turbo pumping experiments. The pumping durations and number of samples for each ice core section are detailed in Table 1.



Table 1. Information for pumping experiments

Ice core section	Pumping duration (min)				
	<i>Rotary pumping experiments (turbo pumping for 10 min)</i>				
NJ-1 (4 samples)	0.5*	9	17	30	
NJ-3 (4 samples)	0.5*	25	60	90	
<i>Turbo pumping experiments (rotary pumping for 0.5 min)</i>					
NJ-2 (5 samples)	10*	20	40	60	90
NJ-4 (5 samples)	3	10*	30	50	90

Note: * denotes the “initial sample” for each ice core section.

155

Table 2. All data summary

Sample ID	Pump time (min)	TAC (scc/g)	Gravitational corrected data			Pair differences with the initial sample				Gas-loss corrected
			$\delta^{18}\text{O}_{\text{grav}}$ (‰)	$\delta\text{O}_2/\text{N}_2_{\text{grav}}$ (‰)	$\delta\text{Ar}/\text{N}_2_{\text{grav}}$ (‰)	$\Delta\delta^{15}\text{N}$ (‰)	$\Delta\delta^{18}\text{O}$ (‰)	$\Delta\delta\text{O}_2/\text{N}_2$ (‰)	$\Delta\delta\text{Ar}/\text{N}_2$ (‰)	$\delta^{18}\text{O}_{\text{atm}}$ (‰)
<i>Rough pumping experiments</i>										
NJ-1-1	0.5	0.066	-0.099	13.26	13.53	0.000	0.000	0.00	0.00	0.021
NJ-1-4	9	0.060	-0.092	21.29	21.13	-0.108	0.007	8.03	7.60	0.116
NJ-1-2	17	0.074	-0.100	12.09	12.40	0.029	-0.001	-1.17	-1.13	0.007
NJ-1-3	30	0.046	-0.361	22.96	21.23	0.064	-0.262	9.70	7.70	-0.094
		1σ	± 0.132							± 0.086
NJ-3-3	0.5	0.080	-0.370	23.73	22.74	0.000	0.000	0.00	0.00	-0.116
NJ-3-4	25	0.072	-0.363	18.95	17.76	-0.001	0.007	-4.78	-4.98	-0.149
NJ-3-2	60	0.059	-0.430	29.32	30.14	0.001	-0.060	5.59	7.40	-0.171
NJ-3-6	90	0.060	-0.237	16.41	17.14	-0.014	0.133	-7.32	-5.60	-0.099
		1σ	± 0.081							± 0.033
<i>Turbo pumping experiments</i>										
NJ-2-1	10	0.049	-0.124	8.88	10.17	0.000	0.000	0.00	0.00	-0.073
NJ-2-4	20	0.056	-0.213	23.95	26.22	-0.001	-0.089	15.07	16.05	-0.044
NJ-2-6	40	0.059	-0.193	17.45	19.65	-0.018	-0.069	8.57	9.48	-0.085
NJ-2-5	60	0.051	-0.194	18.42	21.89	-0.056	-0.070	9.54	11.72	-0.111
NJ-2-3	90	0.056	-0.404	25.85	22.30	0.198	-0.280	16.97	12.13	-0.060
		1σ	± 0.105							± 0.025
NJ-4-3	3	0.066	-0.506	31.92	30.64	0.026	0.037	3.76	7.30	-0.165
NJ-4-2	10	0.045	-0.543	28.16	23.34	0.000	0.000	0.00	0.00	-0.143
NJ-4-5	30	0.064	-0.389	23.29	21.19	0.083	0.154	-4.87	-2.15	-0.109
NJ-4-6	50	0.071	-0.364	17.88	16.99	0.069	0.179	-10.28	-6.35	-0.168
NJ-4-4	90	0.062	-0.473	33.05	29.39	0.087	0.070	4.89	6.05	-0.057
		1σ	± 0.076							± 0.046



2.4 Data corrections

Following chemical slope correction and normalization to the concurrent air standard (Severinghaus et al., 2003), isotopic compositions and gas ratios were corrected for gravitational fractionation (Craig et al., 1988; Bender et al., 1995):

$$\delta_{\text{grav}} = \delta_{\text{vs.air}} - \Delta m \cdot \delta^{15}\text{N} \quad (2)$$

where δ_{grav} represents the gravitationally corrected value of $\delta^{18}\text{O}_{\text{grav}}$, $\delta\text{O}_2/\text{N}_2_{\text{grav}}$ and $\delta\text{Ar}/\text{N}_2_{\text{grav}}$, $\delta_{\text{vs.air}}$ is the value corrected versus air. Δm is the mass difference between the relevant gases, which is 2 for $^{18}\text{O}/^{16}\text{O}$, 4 for O_2/N_2 and 12 for Ar/N_2 .

Gas loss effects are typically evaluated by calculating the pair difference between ice samples from the same depth. As we used a horizontal ice core drilled from a single stratigraphic layer (Fig. 2), the original gas ratios and isotopic compositions were considered identical. Therefore, differences in $\delta^{18}\text{O}_{\text{grav}}$, $\delta\text{O}_2/\text{N}_2_{\text{grav}}$ and $\delta\text{Ar}/\text{N}_2_{\text{grav}}$ values within each ice core section after pumping experiments are attributed to pump-induced “gas losses” or post-coring gas loss. For each experiment, pair differences in isotopic and gas ratio compositions were calculated between samples with different pumping durations and the “initial sample” (Table 1):

$$\Delta\delta = \delta_{\text{grav}} - \delta_{\text{grav},0} \quad (3)$$

where $\Delta\delta$ represents $\Delta\delta^{18}\text{O}$, $\Delta\delta^{15}\text{N}$, $\Delta\delta\text{O}_2/\text{N}_2$, or $\Delta\delta\text{Ar}/\text{N}_2$ pair differences, δ_{grav} is the corresponding gravitational corrected value and $\delta_{\text{grav},0}$ is the value for the “initial sample” of that ice core section. All data are presented in Table 2 and Table S1 in supplementary materials.

3 Results and discussion

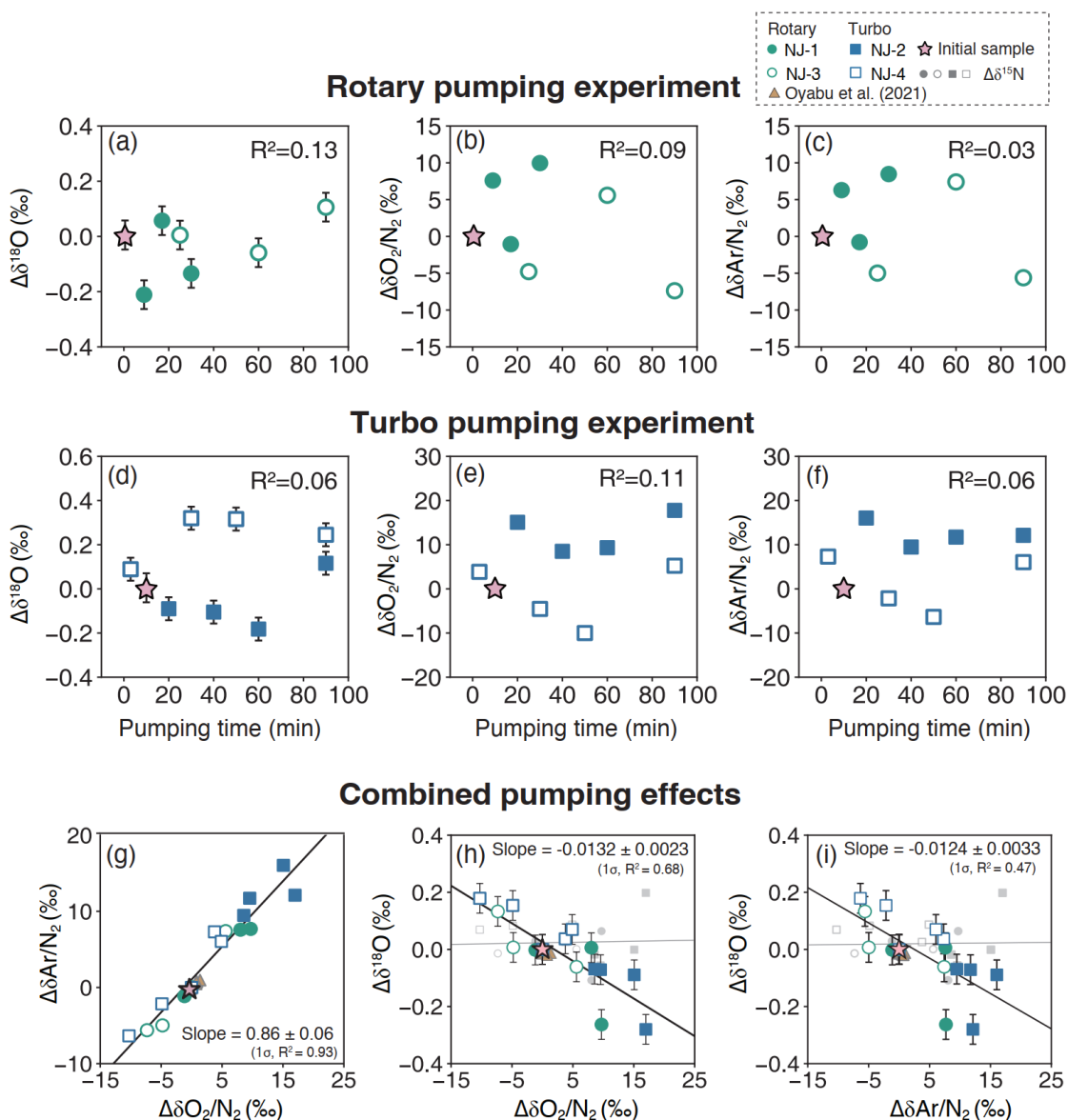
3.1 Gas losses related to pumping duration

Both rotary and turbo pumps operate by compressing gas volume via rotor blades (Song et al., 2004). This process can disturb trapped gases in ice, potentially causing O_2 and Ar leakage. As illustrated in Fig. 1, gas molecules can escape from gas bubbles and diffuse through the ice lattice and microcracks to the exterior. These gas loss processes lead to depletions in $\delta\text{O}_2/\text{N}_2_{\text{grav}}$ and $\delta\text{Ar}/\text{N}_2_{\text{grav}}$, and enrichment in $\delta^{18}\text{O}_{\text{grav}}$ values.

If pump-induced gas loss increased with pumping duration, we would expect a systematic increase in $\Delta\delta^{18}\text{O}$ and decrease in $\Delta\delta\text{O}_2/\text{N}_2$ and $\Delta\delta\text{Ar}/\text{N}_2$ with longer pumping time. However, we observed no clear correlations between pumping duration and $\Delta\delta^{18}\text{O}$, $\Delta\delta\text{O}_2/\text{N}_2$ or $\Delta\delta\text{Ar}/\text{N}_2$ (Fig. 4). For example, the $\Delta\delta^{18}\text{O}$ values for section NJ-2 first decreased and then increased with pumping time, while the parallel experiment on section NJ-4 showed the opposite trend (Fig. 4d). Furthermore, some samples with longer pumping durations exhibited negative $\Delta\delta^{18}\text{O}$ and positive $\Delta\delta\text{O}_2/\text{N}_2$ and $\Delta\delta\text{Ar}/\text{N}_2$ values, indicating less gas losses than the initial sample. These observations contradict the hypothesis that gas losses increase with pumping duration. Oyabu et al. (2021) evacuated Dome Fuji bubbly ice (446.4 m) and clathrate hydrate ice (2001.1 m) samples for 20 min to 5 h. Their observations are consistent with ours: there are either no clear relationships



between pumping time and $\delta^{18}\text{O}$, $\delta\text{O}_2/\text{N}_2$, or $\delta\text{Ar}/\text{N}_2$ for the Dome Fuji ice core (Figure B2 in Oyabu et al., 2021). Therefore, the extent of gas loss is likely not directly related to pumping duration during ice core sample preparation.



190

195

Figure 4: Isotopic and gas ratio variations for pumping experiments. Top row: (a) $\Delta\delta^{18}\text{O}$, (b) $\Delta\delta\text{O}_2/\text{N}_2$, and (c) $\Delta\delta\text{Ar}/\text{N}_2$ variations with pumping time for the rotary pumping experiment. Middle row: (d) $\Delta\delta^{18}\text{O}$, (e) $\Delta\delta\text{O}_2/\text{N}_2$, and (f) $\Delta\delta\text{Ar}/\text{N}_2$ variations with pumping time for the turbo pumping experiment. Bottom row: Cross plots of (g) $\Delta\delta\text{Ar}/\text{N}_2$ – $\Delta\delta\text{O}_2/\text{N}_2$; (h) $\Delta\delta^{18}\text{O}$ – $\Delta\delta\text{O}_2/\text{N}_2$; (i) $\Delta\delta^{18}\text{O}$ – $\Delta\delta\text{Ar}/\text{N}_2$ showing correlations between gas ratios and oxygen isotopic compositions after pumping experiments. NJ-1 (filled green dots) and NJ-3 (open green dots) were used for rotary pumping experiments, while NJ-2 (filled blue squares) and NJ-4 (open blue squares) were used for turbo pumping experiments. Stars denote the “initial sample” for each experiment. $\delta^{15}\text{N}$ data are shown as grey symbols for comparison. We also processed the pumping experiments data in Oyabu et al. (2021) and plotted against our data (yellow triangles in g, h and i). The slopes from their pumping experiments are shown in Table 3. Note that the slopes shown in Figure 4 were calculated only using data from this study.



200

We did observe different magnitudes of gas loss between rotary and turbo pumping experiments. The $\Delta\delta^{18}\text{O}$ values ranged from -0.262 to 0.133 ‰ for rotary pumping and from -0.280 to 0.179 ‰ for turbo pumping experiments (Fig. 4a, d). For rotary pumping experiments, $\Delta\delta\text{O}_2/\text{N}_2$ and $\Delta\delta\text{Ar}/\text{N}_2$ ranged from -7.32 to 9.70 ‰ and -5.60 to 7.70 ‰, respectively (Fig. 4b, c). Whereas for turbo pumping experiments, the ranges were wider: -10.28 to 16.97 ‰ for $\Delta\delta\text{O}_2/\text{N}_2$ and -6.35 to 205 16.05 ‰ for $\Delta\delta\text{Ar}/\text{N}_2$ (Fig. 4e, f). The total variations in $\Delta\delta^{18}\text{O}_{\text{atm}}$ for both pumping experiments are similar, whereas variations in $\Delta\delta\text{O}_2/\text{N}_2$ and $\Delta\delta\text{Ar}/\text{N}_2$ were approximately 1.6 times greater after turbo pumping, suggesting stronger disturbances to trapped gases caused by turbo pump.

In the Oyabu et al. (2021) experiments, the variations in isotopic and gas ratios were much smaller than ours (e.g., ~ 0.02 ‰ for $\Delta\delta^{18}\text{O}$ and < 1 ‰ for gas ratios). This is likely due to the differences in ice quality, i.e. the Dome Fuji ice core is 210 well-preserved and less fractured. Pressure release during drilling and storage can create random microcracks in ice cores (Ikeda-Fukazawa et al., 2005; Kobashi et al., 2008), making fractured ice more susceptible to pump-induced disturbance and gas loss.

3.2 Gas and isotopic fractionations induced by pumping

$\delta\text{O}_2/\text{N}_2$ and $\delta\text{Ar}/\text{N}_2$ values are useful indicators for gas loss, with lower values indicating greater losses (Severinghaus 215 et al., 2009; Extier et al., 2018). Therefore, we used $\Delta\delta\text{O}_2/\text{N}_2$ and $\Delta\delta\text{Ar}/\text{N}_2$ to evaluate the degree of gas losses for each ice sample. In Fig. 4g, we observed strong linear correlations between $\Delta\delta\text{Ar}/\text{N}_2$ and $\Delta\delta\text{O}_2/\text{N}_2$, indicating simultaneous O_2 and Ar losses through ice lattice and cracks. The slopes between $\Delta\delta\text{Ar}/\text{N}_2$ and $\Delta\delta\text{O}_2/\text{N}_2$ were 0.90 and 0.82 for rotary and turbo pumping, respectively (Table 3). These slopes are significantly higher than the ≤ 0.5 slopes typical of BCGL and PCGL. Instead, they were close to the slope of ~ 1 for size-dependent gas losses via lattice diffusion (Fig. 1). We also calculated the 220 paired differences from the Oyabu et al. (2021) pumping experiments using Eq. (3) and plotted against our data (Figure 4). Their $\Delta\delta\text{Ar}/\text{N}_2 - \Delta\delta\text{O}_2/\text{N}_2$ slopes were 0.72 for bubbly ice and 0.86 for clathrate (Table 3), consistent with our observations.

We propose that pumping preferentially disturbs gases within ice fractures rather than those in ice bubbles or the ice lattice. Gases in cracks were preferentially evacuated during pumping, leaving behind bubble-resident gases that have been fractionated by lattice diffusion. The $\Delta\delta\text{Ar}/\text{N}_2$ and $\Delta\delta\text{O}_2/\text{N}_2$ values of these residual gases thus carry a size-dependent 225 fractionation signature, producing slopes near 1. This explains the high slopes we observed.

Pumping also induced oxygen isotopic fractionation. We found that $\Delta\delta^{18}\text{O}$ increased with decreasing $\Delta\delta\text{O}_2/\text{N}_2$ and $\Delta\delta\text{Ar}/\text{N}_2$, while $\Delta\delta^{15}\text{N}$ remained insensitive to gas loss due to the larger molecular diameter of N_2 (Fig. 4h, i). The isotopic fractionation slopes for $\Delta\delta^{18}\text{O} - \Delta\delta\text{O}_2/\text{N}_2$ and $\Delta\delta^{18}\text{O} - \Delta\delta\text{Ar}/\text{N}_2$ were similar for both pump types (Table 3). In a standard sample preparation protocol, an ice sample is evacuated by both pumps. Given the similar fractionation slopes for both pump 230 types, we combined all data to determine the characteristic pump-induced gas and isotopic fractionation slopes. The overall slopes were 0.86 for $\Delta\delta\text{Ar}/\text{N}_2 - \Delta\delta\text{O}_2/\text{N}_2$, -0.0132 ‰·‰⁻¹ for $\Delta\delta^{18}\text{O} - \Delta\delta\text{O}_2/\text{N}_2$ and -0.0124 ‰·‰⁻¹ for $\Delta\delta^{18}\text{O} - \Delta\delta\text{Ar}/\text{N}_2$ (p



< 0.05, Fig. 4). Compared to BCGL and PCGL, pump-induced gas loss has a higher $\Delta\delta\text{Ar}/\text{N}_2 - \Delta\delta\text{O}_2/\text{N}_2$ slope and more negative $\Delta\delta^{18}\text{O} - \Delta\delta\text{O}_2/\text{N}_2$ and $\Delta\delta^{18}\text{O} - \Delta\delta\text{Ar}/\text{N}_2$ slopes (Table 3). These slopes are steeper than those of BCGL and PCGL, indicating greater isotopic fractionation caused by pumping, increasing data scatter. Slopes calculated using processed data of Dome Fuji pumping experiments from Oyabu et al. (2021) also show more significant oxygen isotopic fractionations (Table 3). Although the horizontal ice core used in this study was retrieved from surface of an ice stream, the gas ratio and isotopic fractionation slopes induced by pumping from our experiments and Dome Fuji pumping experiments are similar. This indicates that the gas losses during pumping probably follow similar mechanisms for shallow and deep ice cores.

Our results demonstrate that pump-induced gas loss exhibits a size-dependent fractionation signature for O_2 and Ar and causes greater oxygen isotopic fractionation than BCGL and PCGL. Since pumping primarily affects gases in ice cracks, fractured ice is more susceptible to pump-induced gas loss, increasing the uncertainty in gas ratio and isotopic data. Microcracks develop in all ice cores during drilling, pressure release, and storage (Ikeda-Fukazawa et al., 2005; Kobashi et al., 2008). Minimizing pump influence is therefore crucial, especially for fractured ice like shallow Antarctic blue ice samples. Therefore, pump-induced fractionation is a universal artifact whose magnitude scales with ice quality, but its potential impact exists across all ice core types. To optimize the pumping process, we recommend conducting evacuation tests on empty flasks to determine the minimum time required to reach the critical vacuum pressure. Once the critical vacuum pressure is reached, it is not essential to pump for longer. Instead, reducing unnecessary pumping could possibly minimize the risk of excessive gas losses and isotopic fractionation.

Table 3. Compilation of gas loss fractionation slopes from different studies

Site name	Zone	$\Delta\delta\text{Ar}/\text{N}_2$ vs. $\Delta\delta\text{O}_2/\text{N}_2$ (‰‰ ⁻¹)	1σ	$\Delta\delta^{18}\text{O}_{\text{atm}}$ vs. $\Delta\delta\text{O}_2/\text{N}_2$ (‰‰ ⁻¹)	$\Delta\delta^{18}\text{O}_{\text{atm}}$ vs. $\Delta\delta\text{Ar}/\text{N}_2$ (‰‰ ⁻¹)	References
Pumping gas loss						
oiw2-2	Bubbly ice (rotary)	0.90	0.07	-0.0142	-0.0138	This study
oiw2-2	Bubbly ice (turbo)	0.82	0.08	-0.0140	-0.0142	This study
	Combined	0.86	0.06	-0.0132	-0.0124	This study
Dome Fuji	Bubbly ice (446.4m)	0.72	0.08	-0.0098 ($R^2=0.36$)	-0.0129 ($R^2=0.36$)	Oyabu et al. (2021)
Dome Fuji	Clathrate (2001.1m)	0.86	0.29	-0.0518 ($R^2=0.19$)	-0.0712 ($R^2=0.35$)	Oyabu et al. (2021)
Natural gas loss						
Byrd	All depths (145-2101m)	0.42	0.04	-0.0023 (>1700m)	-0.0037 (>1700m)	Bender et al. (1995)
Vostok-3G	All depths (140-2058m)	0.41	0.06			Bender et al. (1995)
Dome C	Bubbly ice (181-625m)	0.24	0.03			Bender et al. (1995)
Siple Dome	Bubbly ice (75-973m)	0.54	0.01	-0.0065	-0.0035	Severinghaus et al. (2009)
Dome Fuji	Bubbly ice (112-450m)	0.53	0.08	-0.0068	-0.0079	Oyabu et al. (2021)
Dome Fuji	Outer pieces vs. inner pieces	0.22	0.01	-0.0083		Oyabu et al. (2021)



3.3 Gas loss corrections

The strong correlations between $\Delta\delta^{18}\text{O}$ and gas ratios ($\Delta\delta\text{O}_2/\text{N}_2$, $\Delta\delta\text{Ar}/\text{N}_2$) demonstrate that oxygen isotopic fractionation is coupled to the loss of both O_2 and Ar. This highlights the necessity of correcting $\delta^{18}\text{O}_{\text{grav}}$ for gas loss effects
 255 by accounting variations in both $\Delta\delta\text{O}_2/\text{N}_2$ and $\Delta\delta\text{Ar}/\text{N}_2$. By cross-plotting $\Delta\delta^{18}\text{O}$, $\Delta\delta\text{O}_2/\text{N}_2$ and $\Delta\delta\text{Ar}/\text{N}_2$, we calculated the best fit using a multivariate regression model. Therefore, $\delta^{18}\text{O}_{\text{atm}}$ could be corrected using the following equation regarding pump-induced gas losses:

$$\delta^{18}\text{O}_{\text{atm}} = \delta^{18}\text{O}_{\text{grav}} - (-0.037 \cdot \delta\text{O}_2/\text{N}_{2,\text{grav}} + 0.027 \cdot \delta\text{Ar}/\text{N}_{2,\text{grav}}) \quad (4)$$

The gas-loss corrected $\delta^{18}\text{O}_{\text{atm}}$ values are presented in Table 2. We compared the pooled standard deviations of $\delta^{18}\text{O}_{\text{grav}}$ and
 260 $\delta^{18}\text{O}_{\text{atm}}$ for the four pumping experiment datasets (NJ-1 to NJ-4) before and after correction. The pooled standard deviation in $\delta^{18}\text{O}_{\text{atm}}$ decreased from 0.100‰ to 0.051‰, representing about 50% reduction in data scatter. This marked improvement demonstrates that our correction method effectively mitigates pump-induced fractionation and enhances the precision of trapped gas measurements.

As discussed above, pumping primarily evacuates gases residing in ice cracks, while gases trapped within the ice
 265 lattice and bubbles remain largely unaffected. This mechanism explains the high $\Delta\delta\text{Ar}/\text{N}_2 - \Delta\delta\text{O}_2/\text{N}_2$ slope of 0.86 observed in our experiments. The coupled variations of O_2 and Ar in both ice cracks and lattice further inspires a rationale correction of $\delta\text{O}_2/\text{N}_2$ using $\delta\text{Ar}/\text{N}_2$. $\delta\text{O}_2/\text{N}_2$ in BCTZ or clathrate hydrate zone usually exhibit large scatter due to gas diffusion during the bubble to clathrate transition (Bender 2002; Ikeda-Fukazawa et al., 2005; Landais et al., 2012). Gas loss effects in these zones can be evaluated similarly using the $\Delta\delta\text{Ar}/\text{N}_2 - \Delta\delta\text{O}_2/\text{N}_2$ relationship derived from paired samples at the same depth.

270 Based on the strong correlation between O_2 and Ar, $\delta\text{O}_2/\text{N}_2$ could be corrected using $\delta\text{Ar}/\text{N}_2$ as an indicator of gas loss:

$$\delta\text{O}_2/\text{N}_{2,\text{corr}} = \delta\text{O}_2/\text{N}_{2,\text{grav}} - m \cdot \delta\text{Ar}/\text{N}_{2,\text{grav}} \quad (5)$$

where m is the slope of the $\Delta\delta\text{Ar}/\text{N}_2 - \Delta\delta\text{O}_2/\text{N}_2$ relationship for a given ice core section, $\delta\text{O}_2/\text{N}_{2,\text{corr}}$ is the gas loss corrected value. We applied this correction method to gas ratio data from the BCTZ and upper clathrate hydrate zone of the Dome Fuji ice core (450-1500 m), where previous measurements showed pronounced scatter in $\delta\text{O}_2/\text{N}_2$ and $\delta\text{Ar}/\text{N}_2$. We divided these
 275 samples into three depth intervals: upper BCTZ (450-800 m), lower BCTZ (800-1200 m) and upper clathrate hydrate zone (1200-1450 m). The $\Delta\delta\text{Ar}/\text{N}_2 - \Delta\delta\text{O}_2/\text{N}_2$ slopes for these three intervals are 0.6066, 0.8939, and 0.5252, respectively. After correcting the $\delta\text{O}_2/\text{N}_2$ values using equation (5), the residuals of $\delta\text{O}_2/\text{N}_{2,\text{corr}}$ relative to a low-pass-filtered curve substantially reduced compared to the original data in Oyabu et al. (2021) (Fig. 5). The low-pass-filtered curve is designed by linear interpolating $\delta\text{O}_2/\text{N}_2$ data at 0.1-kyr intervals with a cut-off period from 16.7 to 10.0 kyr, same as Kawamura et al. (2007).
 280 This marked reduction in scatter demonstrates that our correction method can effectively recover coherent orbital-scale signals from noisy $\delta\text{O}_2/\text{N}_2$ records in the BCTZ, enhancing the fidelity of orbital tuning dating of deep ice cores.

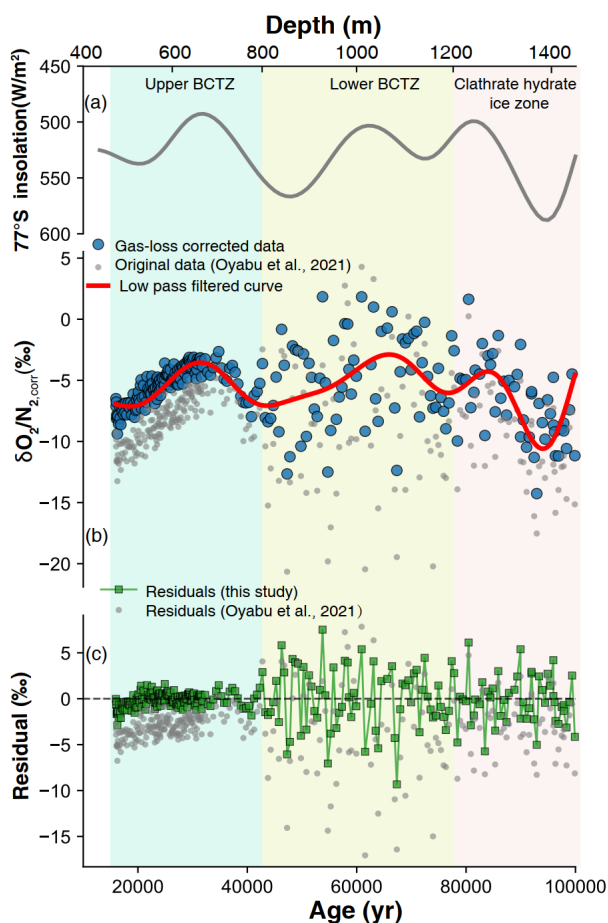


Figure 5: Gas-loss corrected $\delta\text{O}_2/\text{N}_2$ records from the BCTZ and upper clathrate hydrate zone of Dome Fuji ice core plotted against ice age and depth. (a) Summer insolation at 77°S (W m^{-2} ; Laskar et al., 2004). (b) Gas-loss corrected $\delta\text{O}_2/\text{N}_2$ corr data (blue dots) with corresponding low-pass filtered curves (red lines; filter using parameters same as Kawamura et al. 2007). Gray dots show the original $\delta\text{O}_2/\text{N}_2$ grav data from Oyabu et al. (2021). (c) Absolute residuals between the $\delta\text{O}_2/\text{N}_2$ corr and their low-pass filtered curves. Green squares represent residuals calculated in this study; grey dots represent residuals from Oyabu et al. (2021). Shaded regions denote the Upper BCTZ (450–800 m), Lower BCTZ (800–1200 m), and upper clathrate hydrate ice zone (1200–1450 m).

285

290 4 Conclusions

Our experiments provide the first quantitative constraints on pump-induced fractionation during ice core gas extraction, revealing mechanistic pathways distinct from BCGL and PCGL. The $\Delta\delta\text{Ar}/\text{N}_2 - \Delta\delta\text{O}_2/\text{N}_2$ slope of 0.86 confirms the dominance of size-dependent fractionation in remaining gases after pumping. This can be attributed to the selective evacuation of fracture-hosted gases, leaving bubble-resident gases fractionated by lattice diffusion. Isotopic enrichment in $\Delta\delta^{18}\text{O}$ correlated strongly with gas loss magnitude, yielding fractionation slopes of $-0.0132\text{‰}\cdot\text{‰}^{-1}$ against $\Delta\delta\text{O}_2/\text{N}_2$ and $-0.0124\text{‰}\cdot\text{‰}^{-1}$ against $\Delta\delta\text{Ar}/\text{N}_2$, substantially steeper than those associated with natural gas loss processes. The partial removal of fracture-hosted gases introduces larger apparent $\delta^{18}\text{O}_{\text{atm}}$ fractionations compared to BCGL and PCGL, increasing data uncertainties.

295



The strong correlations between $\Delta\delta^{18}\text{O}$ and gas ratios demonstrate that oxygen isotopic fractionation is coupled to the loss of both O_2 and Ar.

300 The magnitude of gas loss varied randomly across ice core sections and showed no correlation with pumping duration, but was consistently greater for turbo pumping than rotary pumping. The concurrent loss of O_2 , Ar and lighter isotopes indicate gas loss through ice microcracks during pumping. These findings underscore that fractured ice, common in shallow Antarctic blue ice, brittle ice or poorly preserved ice cores, is highly vulnerable to pump artifacts. Shortening evacuation time after achieving critical vacuum pressure is recommended for these ice cores.

305 Critically, we demonstrate that pump-induced fractionation can be effectively corrected. Our O_2 -Ar coupled multivariate correction reduces the pooled standard deviation of $\delta^{18}\text{O}_{\text{atm}}$ by $\sim 50\%$, from 0.100‰ to 0.051‰. More importantly, applying a $\delta\text{Ar}/\text{N}_2$ -based correction to the Dome Fuji ice core substantially reduces scatter in $\delta\text{O}_2/\text{N}_2$ records from the BCTZ, enabling recovery of coherent orbital-scale signals essential for accurate ice core chronology. This marks the demonstration that gas loss artifacts in this challenging depth interval can be systematically corrected, with direct implications for orbital
310 tuning and paleoclimate reconstruction.

Data availability

All data are presented in the main text and have been deposited to Figshare (<https://doi.org/10.6084/m9.figshare.30674912>).

Author contribution

315 QL conducted the pumping experiments, measured the ice core trapped gases, and wrote the original manuscript. HH conceived the idea of this study and interpreted the data. HH and GS reviewed and edited the manuscript. GS, DW and ZL conducted the ice core drilling. HH, GS and SH provided financial support to this study.

Competing interests

The authors declare that they have no conflict of interest.

320 Acknowledgement

We thank Michael L. Bender for his mentoring, manuscript review, and financial support. We thank Ikumi Oyabu for sharing the pumping experiments data of the Dome Fuji ice core, and thank Yuzhen Yan for thoughtful discussions.

Financial support



This work was supported by the National Key Research and Development Program of China (2024YFC2816803), the
325 National Natural Science Foundation of China (42576284 and 42276243) and the Shanghai Frontiers Science Center of Polar
Science (SCOPS).

References

- Andree, M., Beer, J., Loetscher, H. P., Moor, E., Oeschger, H., Bonani, G., Hofmann, H. J., Morenzoni, E., Nenni, M., and
330 Suter, M.: Dating Polar Ice by ^{14}C Accelerator Mass Spectrometry, *Radiocarbon*, 28, 417-423,
<https://doi.org/10.1017/S0033822200007530>, 1986.
- Bender, M., Sowers, T., and Lipenkov, V.: On the concentrations of O_2 , N_2 , and Ar in trapped gases from ice cores, *Journal of
Geophysical Research-Atmospheres*, 100, 18651-18660, <https://doi.org/10.1029/94jd02212>, 1995.
- Bender, M. L.: Orbital tuning chronology for the Vostok climate record supported by trapped gas composition, *Earth and
Planetary Science Letters*, 204, 275-289, [https://doi.org/10.1016/S0012-821X\(02\)00980-9](https://doi.org/10.1016/S0012-821X(02)00980-9), 2002.
- 335 Craig, H., Horibe, Y., and Sowers, T.: Gravitational Separation of Gases and Isotopes in Polar Ice Caps, *Science*, 242, 1675-
1678, <https://doi.org/10.1126/science.242.4886.1675>, 1988.
- Emerson, S., Quay, P. D., Stump, C., Wilbur, D., and Schudlich, R.: CHEMICAL TRACERS OF PRODUCTIVITY AND
RESPIRATION IN THE SUBTROPICAL PACIFIC-OCEAN, *Journal of Geophysical Research-Oceans*, 100, 15873-
15887, <https://doi.org/10.1029/95jc01333>, 1995.
- 340 Extier, T., Landais, A., Bréant, C., Prié, F., Bazin, L., Dreyfus, G., Roche, D. M., and Leuenberger, M.: On the use of $\delta^{18}\text{O}_{\text{atm}}$
for ice core dating, *Quaternary Science Reviews*, 185, 244-257, <https://doi.org/10.1016/j.quascirev.2018.02.008>, 2018.
- Higgins, J. A., Kurbatov, A. V., Spaulding, N. E., Brook, E., Introne, D. S., Chimiak, L. M., Yan, Y., Mayewski, P. A., and
Bender, M. L.: Atmospheric composition 1 million years ago from blue ice in the Allan Hills, Antarctica, *Proceedings of
the National Academy of Sciences of the United States of America*, 112, 6887-6891,
345 <https://doi.org/10.1073/pnas.1420232112>, 2015.
- Hu, H. T., Li, Q. Y., Zhang, W. B., Wu, S. Y., Song, J., Liu, K., Zou, X., Pang, H. X., Yan, M. J., and Hou, S. G.: $\delta^{18}\text{O}$ of O_2
in a Tibetan ice core constrains Its chronology to the Holocene, *Geophysical Research Letters*, 49,
<https://doi.org/10.1029/2022gl098368>, 2022.
- 350 Huber, C., Beyerle, U., Leuenberger, M., Schwander, J., Kipfer, R., Spahni, R., Severinghaus, J. P., and Weiler, K.: Evidence
for molecular size dependent gas fractionation in firm air derived from noble gases, oxygen, and nitrogen measurements,
Earth and Planetary Science Letters, 243, 61-73, <https://doi.org/10.1016/j.epsl.2005.12.036>, 2006.
- Ikedo-Fukazawa, T., Fukumizu, K., Kawamura, K., Aoki, S., Nakazawa, T., and Hondoh, T.: Effects of molecular diffusion
on trapped gas composition in polar ice cores, *Earth and Planetary Science Letters*, 229, 183-192,
<https://doi.org/10.1016/j.epsl.2004.11.011>, 2005.
- 355 Jouzel, J., Masson-Delmotte, V., Cattani, O., Dreyfus, G., Falourd, S., Hoffmann, G., Minster, B., Nouet, J., Barnola, J. M.,
Chappellaz, J., Fischer, H., Gallet, J. C., Johnsen, S., Leuenberger, M., Loulergue, L., Luethi, D., Oerter, H., Parrenin,
F., Raisbeck, G., Raynaud, D., Schilt, A., Schwander, J., Selmo, E., Souchez, R., Spahni, R., Stauffer, B., Steffensen, J.
P., Stenni, B., Stocker, T. F., Tison, J. L., Werner, M., and Wolff, E. W.: Orbital and Millennial Antarctic Climate
Variability over the Past 800,000 Years, *Science*, 317, 793-796, <https://doi.org/10.1126/science.1141038>, 2007.
- 360 Kawamura, K., Parrenin, F., Lisiecki, L., Uemura, R., Vimeux, F., Severinghaus, J. P., Hutterli, M. A., Nakazawa, T., Aoki,
S., and Jouzel, J.: Northern Hemisphere forcing of climatic cycles in Antarctica over the past 360,000 years, *Nature*,
448, 912-916, <https://doi.org/10.1038/nature06015>, 2007.
- Kobashi, T., Severinghaus, J. P., and Kawamura, K.: Argon and nitrogen isotopes of trapped air in the GISP2 ice core during
the Holocene epoch (0-11,500 B.P.): Methodology and implications for gas loss processes, *Geochimica Et
Cosmochimica Acta*, 72, 4675-4686, <https://doi.org/10.1016/j.gca.2008.07.006>, 2008.
- 365 Landais, A., Dreyfus, G., Capron, E., Pol, K., Loutre, M. F., Raynaud, D., Lipenkov, V. Y., Arnaud, L., Masson-Delmotte, V.,
Paillard, D., Jouzel, J., and Leuenberger, M.: Towards orbital dating of the EPICA Dome C ice core using $\delta\text{O}_2/\text{N}_2$,
Climate of the Past, 8, 191-203, <https://doi.org/10.5194/cp-8-191-2012>, 2012.



- 370 Laskar, J., Robutel, P., Joutel, F., Gastineau, M., Correia, A. C. M., and Levrard, B.: A long-term numerical solution for the insolation quantities of the Earth, *Astron. Astrophys.*, 428, 261–285, <https://doi.org/10.1051/0004-6361:20041335>, 2004.
- Oyabu, I., Kawamura, K., Uchida, T., Fujita, S., Kitamura, K., Hirabayashi, M., Aoki, S., Morimoto, S., Nakazawa, T., Severinghaus, J. P., and Morgan, J. D.: Fractionation of O₂/N₂ and Ar/N₂ in the Antarctic ice sheet during bubble formation and bubble-clathrate hydrate transition from precise gas measurements of the Dome Fuji ice core, *Cryosphere*, 15, 5529–5555, <https://doi.org/10.5194/tc-15-5529-2021>, 2021.
- 375 Petit, J. R., Jouzel, J., Raynaud, D., Barkov, N. I., Barnola, J. M., Basile, I., Bender, M., Chappellaz, J., Davis, M., Delaygue, G., Delmotte, M., Kotlyakov, V. M., Legrand, M., Lipenkov, V. Y., Lorius, C., Pépin, L., Ritz, C., Saltzman, E., and Stievenard, M.: Climate and atmospheric history of the past 420,000 years from the Vostok ice core, Antarctica, *Nature*, 399, 429–436, <https://doi.org/10.1038/20859>, 1999.
- 380 Reid, R. C., Sherwood, T. K., and Street, R. E.: The Properties of Gases and Liquids, *Physics Today*, 12, 38–40, <https://doi.org/10.1063/1.3060771>, 1959.
- Seltzer, A. M., Buizert, C., Baggenstos, D., Brook, E. J., Ahn, J., Yang, J. W., and Severinghaus, J. P.: Does $\delta^{18}\text{O}$ of O₂ record meridional shifts in tropical rainfall?, *Climate of the Past*, 13, 1323–1338, <https://doi.org/10.5194/cp-13-1323-2017>, 2017.
- 385 Severinghaus, J. P.: South Pole (SPICECORE) ¹⁵N, ¹⁸O, O₂/N₂ and Ar/N₂ (Version 1) [dataset], <https://doi.org/10.15784/601152>, 2019.
- Severinghaus, J. P. and Battle, M. O.: Fractionation of gases in polar ice during bubble close-off: New constraints from firm air Ne, Kr and Xe observations, *Earth & Planetary Science Letters*, 244, 474–500, <https://doi.org/10.1016/j.epsl.2006.01.032>, 2006.
- 390 Severinghaus, J. P., Grachev, A., Luz, B., and Caillon, N.: A method for precise measurement of argon 40/36 and krypton/argon ratios in trapped air in polar ice with applications to past firm thickness and abrupt climate change in Greenland and at Siple Dome, Antarctica, *Geochimica Et Cosmochimica Acta*, 67, 325–343, [https://doi.org/10.1016/S0016-7037\(02\)00965-1](https://doi.org/10.1016/S0016-7037(02)00965-1), 2003.
- Severinghaus, J. P., Beaudette, R., Headly, M. A., Taylor, K., and Brook, E. J.: Oxygen-18 of O₂ Records the Impact of Abrupt Climate Change on the Terrestrial Biosphere, *Science*, 324, 1431–1434, <https://doi.org/10.1126/science.1169473>, 2009.
- 395 Severinghaus, J. P., Sowers, T., Brook, E. J., Alley, R. B., and Bender, M. L.: Timing of abrupt climate change at the end of the Younger Dryas interval from thermally fractionated gases in polar ice, *Nature*, 391, 141–146, <https://doi.org/10.1038/34346>, 1998.
- 400 Shackleton, S., Hishamunda, V., Davidge, L., Brook, E., Peterson, J. M., Carter, A., Aarons, S., Kurbatov, A., Introne, D., Yan, Y., Nesbitt, I. M., Buizert, C., Steig, E. J., Schauer, A. J., Morgan, J., Neff, P. D., Epifanio, J. A., Severinghaus, J., Bender, M., and Higgins, J. A.: Miocene and Pliocene ice and air from the Allan Hills blue ice area, East Antarctica, *Proceedings of the National Academy of Sciences of the United States of America*, 122(44), e2502681122, <https://doi.org/10.1073/pnas.2502681122>, 2025.
- 405 Song, C.-A., J. F. S., and -E. Q. L.: Experimental study on obtaining high vacuum by molecular pump, *Gansu Science and Technology*, 113–115, 2004.
- Sowers, T., Bender, M., and Raynaud, D.: Elemental and isotopic composition of occluded O₂ and N₂ in polar ice, *Journal of Geophysical Research*, 94, 5137, <https://doi.org/10.1029/JD094iD04p05137>, 1989.
- 410 Sowers, T., Brook, E., Etheridge, D., Blunier, T., Fuchs, A., Leuenberger, M., Chappellaz, J., Barnola, J. M., Wahlen, M., and Deck, B.: An interlaboratory comparison of techniques for extracting and analyzing trapped gases in ice cores, *Journal of Geophysical Research Oceans*, 102, 26527–26538, <https://doi.org/10.1029/97JC00633>, 1997.
- Stolper, D. A., Bender, M. L., Dreyfus, G. B., Yan, Y., and Higgins, J. A.: A Pleistocene ice core record of atmospheric O₂ concentrations, *Science*, 353, 1427–1430, <https://doi.org/10.1126/science.aaf5445>, 2016.
- 415 Suwa, M. and Bender, M. L.: Chronology of the Vostok ice core constrained by O₂/N₂ ratios of occluded air, and its implication for the Vostok climate records, *Quaternary Science Reviews*, 27, 1093–1106, <https://doi.org/10.1016/j.quascirev.2008.02.017>, 2008.
- Wilson, A. T. and Donahue, D. J.: THE RECOVERY AND DATING OF CARBON-DIOXIDE IN POLAR ICE CORES, *Radiocarbon*, 31, 579–584, 1989.



- 420 Wilson, A. T. and Long, A.: New approaches to CO₂ analysis in polar ice cores, *Journal of Geophysical Research-Oceans*,
102, 26601-26606, <https://doi.org/10.1029/97jc00159>, 1997.
- Yan, Y. Z., Bender, M. L., Brook, E. J., Clifford, H. M., Kemeny, P. C., Kurbatov, A. V., Mackay, S., Mayewski, P. A., Ng, J.,
Severinghaus, J. P., and Higgins, J. A.: Two-million-year-old snapshots of atmospheric gases from Antarctic ice, *Nature*,
574, 663-+, <https://doi.org/10.1038/s41586-019-1692-3>, 2019.
- 425 Yan, Y., Brook, E. J., Kurbatov, A. V., Severinghaus, J. P., and Higgins, J. A.: Ice core evidence for atmospheric oxygen
decline since the Mid-Pleistocene transition, *Science Advances*, 7, eabj9341, <https://doi.org/10.1126/sciadv.abj9341>,
2021.